Dynamical Black Holes and Accretion-Induced Backreaction

Thiago de L. Campos [1], C. Molina [2,*] and Mario C. Baldiotti [3]

1   Instituto de Física, Universidade de São Paulo, Caixa Postal 66318, São Paulo CEP 05315-970, SP, Brazil; thiagocampos@usp.br

2   Escola de Artes, Ciências e Humanidades, Universidade de São Paulo, Avenida Arlindo Bettio 1000, São Paulo CEP 03828-000, SP, Brazil

3   Departamento de Física, Universidade Estadual de Londrina, Londrina CEP 86051-990, PR, Brazil; baldiotti@uel.br

*   Correspondence: cmolina@usp.br

Abstract

We investigate the evolution of future trapping horizons through the dynamics of the Misner–Sharp mass using ingoing Eddington–Finkelstein coordinates. Our analysis shows that an integral formulation of Hayward's first law governs much of the evolution of general spherically symmetric spacetimes. To account for the accretion backreaction, we consider a near-horizon approximation, which yields first-order corrections of a Vaidya-dark energy form. We further propose a systematic perturbative scheme to study these effects for an arbitrary background. As an application, we analyze an accreting Reissner–Nordström black hole and demonstrate the horizon shifts produced. Finally, we compute accretion-induced corrections to an extremal configuration. It is shown that momentum influx and energy density produce distinct effects: the former forces the splitting of the extremal horizon, while the latter induces significant displacements in its position, computed up to first-order perturbative corrections. These results highlight how different components of the stress–energy tensor significantly affect horizon geometry, with potential implications for broader areas of research, including black-hole thermodynamics.

Keywords: dynamical black hole; trapping horizon; Misner–Sharp mass; accretion; backreaction

1. Introduction

Black holes are inherently dynamical systems that interact with their environment through accretion or Hawking evaporation. As horizons evolve and spacetime departs from equilibrium, defining and studying black holes in dynamical regimes requires moving beyond traditional tools like event horizons and Arnowitt-Deser-Misner (ADM)/Komar mass [1,2]. Quasi-local approaches, such as trapping horizons [3] and the Misner–Sharp mass [4], have emerged as essential counterparts in the descriptions of horizon dynamics and gravitational energy without relying on particular asymptotic structures [5–13], and avoiding teleological definitions [14]. Spherically symmetric spacetimes provide an ideal testing ground for these methods, simplifying the analysis of quasi-local quantities while preserving much of the essential phenomenology of gravitational dynamics.

While many exact solutions of the Einstein field equations exist, remarkably few describe dynamically interacting black holes with exact treatment for accretion or evaporation. Notable examples include the McVittie spacetime (and its generalizations) for cosmological black holes [15–20], the Thakurta solution [21], and the Vaidya metric [22,23], which later

extended to include the cosmological constant [24,25]. The scarcity of exact solutions for dynamical black holes makes perturbative and approximate approaches indispensable. These methods are crucial for modeling realistic scenarios, such as the backreaction of accreting matter on the metric tensor. For instance, the perturbative framework developed by Babichev, Dokuchaev, and Eroshenko [26] generates first-order metric corrections arising from the energy–momentum tensor in the test-fluid approximation, with the leading term in a Vaidya-like form.

As we will show, the ingoing Eddington–Finkelstein coordinates not only avoid coordinate singularities typical of black holes but also reveal the dynamics of the Misner–Sharp mass in an intuitive way. This is a feature that is largely exploited in our work to analyze general aspects of the evolution of trapping horizons beyond approximate results. To develop effective descriptions within this framework, with this chart accommodating future outer (FOTH) and inner (FITH) trapping horizons, we first employ an approximation scheme to simplify the line element near a trapping horizon, yielding particularly tractable results for perfect fluids. Building on this, we implement a systematic perturbative expansion that goes beyond first-order corrections of matter-energy influx. A comprehensive analysis of Reissner–Nordström black holes is carried out, with special attention given to the extremal case.

This paper is organized as follows. In Section 2 the general spherically symmetric framework is presented. The dynamics of the Misner–Sharp mass were investigated, with a connection to Hayward's first law established. We show in Section 3 that the metric admits a suitable approximation in the neighborhood of any 2-sphere (here called "Vaidya-dark energy"). We implement this approximation scheme specifically for perfect fluids near the horizon. In Section 4, we introduce our perturbative approach to accretion, systematically examining its effects on trapping horizon displacements. The presence of inner horizons is analyzed in Section 5, with particular emphasis on how repulsive corrections in the Misner–Sharp mass can eliminate a small FITH of a Reissner–Nordström black hole. We conclude with a discussion and outlook in Section 6, with Appendix A providing a concise review of future trapping horizon characterization. In the present work, we use signature $(-+++)$.

2. Dynamics of Spherically Symmetric Spacetimes

2.1. General Setup

This work focuses on a quasi-local approach in spherically symmetric spacetimes. In this framework, the Misner–Sharp mass (M_{MS}), defined as

$$M_{\mathrm{MS}} \equiv \frac{r}{2}(1 - g^{\mu\gamma}\partial_\mu r \partial_\gamma r) \, , \tag{1}$$

can be interpreted as the energy of the system inside a 2-sphere of area $4\pi r^2$ (r denoted as the "areal radius").

To study black holes while avoiding coordinate singularities, one can use ingoing Eddington–Finkelstein coordinates (v, r, θ, ϕ), where v is the so-called "advanced time" (actually a null coordinate). In this chart, a general spherically symmetric spacetime is described by the line element [27]:

$$ds^2 = -e^{2\lambda(v,r)}\left(1 - \frac{2M_{\mathrm{MS}}}{r}\right)dv^2 + 2e^{\lambda(v,r)}dvdr + r^2 d\Omega^2 \, , \quad M_{\mathrm{MS}} \equiv M_{\mathrm{MS}}(v,r) \, . \tag{2}$$

It is straightforward to calculate the Einstein tensor $G_\mu{}^\gamma$, whose relevant components for this work are

$$G_v{}^v = -\frac{2\partial_r M_{\mathrm{MS}}}{r^2} \,, \quad G_v{}^r = \frac{2\partial_v M_{\mathrm{MS}}}{r^2} \,, \quad G_r{}^v = \frac{2e^{-\lambda}\partial_r \lambda}{r} \,. \tag{3}$$

The Einstein equation is

$$G_\mu{}^\gamma = 8\pi\left(T_\mu{}^\gamma - \rho_\Lambda \delta_\mu{}^\gamma\right) \,, \quad G_\mu{}^\gamma \equiv G_\mu{}^\gamma(v,r) \,, \quad T_\mu{}^\gamma \equiv T_\mu{}^\gamma(v,r) \,, \tag{4}$$

where $\rho_\Lambda \equiv \Lambda/8\pi$ denotes the energy density of the vacuum. From the first two components in Equation (3), we obtain

$$\partial_r M_{\mathrm{MS}} = -4\pi r^2 (T_v{}^v - \rho_\Lambda) \,, \quad \partial_v M_{\mathrm{MS}} = 4\pi r^2 T_v{}^r \,. \tag{5}$$

The third component in Equation (3) yields

$$\partial_r e^{-\lambda} = \frac{r}{2} G_r{}^v \,, \tag{6}$$

which can be integrated to

$$e^{-\lambda(v,r)} = 4\pi \int_{r_0}^r T_r{}^v(v,r') r' \, dr' + e^{-\lambda(v,r_0)} \,. \tag{7}$$

Under the coordinate transformation $dv \longrightarrow e^{-\lambda(v,r_0)} dv$, the general line element (2) reads

$$ds^2 = -e^{2\lambda(v,r)-2\lambda(v,r_0)}\left(1 - \frac{2M_{\mathrm{MS}}}{r}\right) dv^2 + 2e^{\lambda(v,r)-\lambda(v,r_0)} dv dr + r^2 d\Omega^2 \,. \tag{8}$$

It is apparent that the general metric, written in the form (8), can be approximated by the Vaidya metric sufficiently close to $r = r_0$. At this stage, r_0 remains an arbitrary parameter.

2.2. Dynamics of the Misner–Sharp Mass

To analyze the evolution of the system, we express the Misner–Sharp mass in terms of convenient dynamical variables, using the differential equations in (5), as

$$M_{\mathrm{MS}}(v,r) - M_{\mathrm{MS}}(0,r_0) = \int_0^v \mathcal{A}(v',r_0) \, dv' + \int_{r_0}^r \mathcal{B}(v,r') \, dr' \,. \tag{9}$$

The flux and energy functions $\mathcal{A}$ and $\mathcal{B}$ are defined as

$$\mathcal{A} \equiv 4\pi r^2 T_v{}^r \,, \quad \mathcal{B} \equiv -4\pi r^2 (T_v{}^v - \rho_\Lambda) \,. \tag{10}$$

These quantities have clear physical interpretations. The term $\mathcal{A}$ generates the radial energy flux through a sphere of radius r at a fixed v, while $\mathcal{B}$ gives the effective energy density within that sphere (including the cosmological constant contribution). In Equation (9), r_0 serves as an arbitrary reference radius that sets the initial condition for the integration. It follows that the evolution of the Misner–Sharp mass in Equation (9) admits the following physical interpretation. For any $v > 0$ and $r > r_0$, the mass consists of three contributions:

- the initial mass at the reference radius r_0;
- the accumulated energy flux through the 2-sphere at r_0 from $v' = 0$ to $v' = v$;
- the final energy contained between the 2-spheres at r_0 and r.

We observe that the Misner–Sharp mass at the reference radius r_0 takes the form

$$M_{\mathrm{MS}}(v, r_0) = M_{\mathrm{MS}}(0, r_0) + \int_0^v \mathcal{A}(v', r_0) \, dv' \,, \tag{11}$$

provided that $\mathcal{B}$ remains finite. The boundness of $\mathcal{B}$ is taken as a physically reasonable assumption for the energy density. Result (11) shows that at $r = r_0$, the mass evolves purely as a function of v, representing an effective Vaidya solution with initial mass $M_{\mathrm{MS}}(0, r_0)$.

Let us assume that our system of interest is a black hole with a singularity at $r \to 0$. Since r_0 is arbitrary in our treatment, we can take the limit $r_0 \to 0$ in (11):

$$M(v) \equiv \lim_{r_0 \to 0} M_{\mathrm{MS}}(0, r_0) + \int_0^v \lim_{r_0 \to 0} \mathcal{A}(v', r_0) \, dv' \,. \tag{12}$$

Therefore, we interpret the mass of the singularity itself as $M(v)$ in Equation (12), which adds its initial mass to all the influx of energy.

Building on Equation (9), we define the total energy of the black hole at time v as the corresponding Misner–Sharp mass:

$$M_{\mathrm{MS}}(v, r_H(v)) \equiv M(v) + \lim_{r_0 \to 0} \int_{r_0}^{r_H(v)} \mathcal{B}(v, r') \, dr' \,, \tag{13}$$

where $r_H(v)$ is the position of the black-hole boundary. This surface constitutes a future trapping horizon, which is the closure of a hypersurface foliated by 2-dimensional surfaces satisfying

$$\theta_l = 0 \,, \quad \theta_n < 0 \,. \tag{14}$$

In Equation (14), θ_l and θ_n are the expansion scalars associated with the outgoing (l^μ) and ingoing (n^ν) congruences, respectively. For its full characterization further conditions must be analyzed (see Appendix A for a short exposition on this subject). We denote a future outer trapping horizon (FOTH) as $r = r_+$, a future inner trapping horizon (FITH) as $r = r_-$, and if it is not specified, we use r_H for the horizon radius.

Similarly to Equation (13), we obtain the Misner–Sharp mass decomposition:

$$M_{\mathrm{MS}}(v, r) = M(v) + \lim_{r_0 \to 0} \int_{r_0}^{r} \mathcal{B}(v, r') \, dr' \,, \tag{15}$$

where $M(v)$ represents the singularity's time-dependent mass. Note that the energy–momentum tensor only determines variations in the Misner–Sharp mass since there is a free integration constant $[M_{\mathrm{MS}}(0, r_0)]$, which must be specified in other ways.

The presented developments are well contextualized in the so-called Hayward thermodynamics [3,28–30], which established a consistent thermodynamic description for evolving black holes and wormholes in non-stationary, spherically symmetric spacetimes. Within this formalism, black holes are defined by their trapping horizons.

This framework allows deeper insights into the dynamics of the Misner–Sharp mass, especially in non-stationary and strongly curved regimes. For instance, M_{MS} can be interpreted as the conserved quantity associated with the conserved current $J^\mu \equiv G^{\mu\gamma} \mathrm{K}_\gamma$ [31], where K^μ is the Kodama vector [32]. Furthermore, the Misner–Sharp mass in Equation (9) leads to a generalized first law of black-hole thermodynamics that has its origins in [29,30]

$$\nabla_\mu M_{\mathrm{MS}} = A \psi_\mu + w \nabla_\mu V \,, \tag{16}$$

where A and V are the Euclidean area and volume of a 2-sphere, and we assume that the relevant quantities can be expressed as functions of (v, r). In Equation (16), the energy-flux vector field (ψ^μ) and work-density scalar (w) are given by

$$\psi^\mu \equiv \frac{1}{8\pi} G^{\mu\gamma} \nabla_\gamma r + w \nabla^\mu r, \qquad w = -\frac{1}{16\pi} g_{ab} G^{ab}, \tag{17}$$

where g_{ab} is the metric on the $(1+1)$-dimensional reduced spacetime orthogonal to the spherical orbits. In the coordinates (v, r),

$$\psi_\mu = \frac{1}{8\pi} G_\mu{}^r + w\delta_\mu{}^r, \qquad w = -\frac{G_v{}^v + G_r{}^r}{16\pi}, \tag{18}$$

with the nonzero components of Equation (16). Thus,

$$\partial_v M_{\mathrm{MS}} = A\psi_v = \mathcal{A}, \qquad \partial_r M_{\mathrm{MS}} = 4\pi r^2 \left(\frac{1}{8\pi} G_r{}^r + 2w \right) = \mathcal{B}. \tag{19}$$

This analysis shows that Equation (9) is an integral form of Equation (16) for the Kodama vector $K^\mu = e^{-\lambda}(\partial_v)^\mu$. Up to this point, there are no approximations involved.

3. Near-Horizon Approximation Scheme

3.1. Existence of Future Trapping Horizons

Following Hayward's approach, we define a black hole in terms of its trapping horizons. More precisely, we assume that the black-hole boundary is a future outer trapping horizon, a concept that is properly reviewed in Appendix A.

Future outer trapping horizons and future inner trapping horizons are characterized (respectively) by the conditions $\mathcal{B}(v, r_+(v)) < 1/2$ and $\mathcal{B}(v, r_-(v)) > 1/2$ on the surface $r = 2M_{\mathrm{MS}}$. The sign of $\mathcal{B}$, and thus the type of horizon, depends on the component $T_v{}^v$ of the energy–momentum tensor and also on the sign and magnitude of the cosmological constant Λ. We initially consider the case of a vanishing Λ and write $T_v{}^v = T^v{}_\mu \delta_v^\mu$. We observe that $T_v{}^v < 0$ in regions where ∂_v is future-directed, assuming the dominant energy condition holds. Hence $\mathcal{B} > 0$ within these assumptions, with large (in module) $T_v{}^v$ contributing to the preferable existence of FITHs. Although the positivity of $\mathcal{B}$ is assured by the dominant energy condition in this case, in regions of $g_{vv} > 0$, the sign of $\mathcal{B}$ is not determined *a priori*. If a cosmological constant is present, a $\Lambda > 0$ also contributes to the formation of FITHs. But that is not the case if $\Lambda < 0$.

Several physically significant solutions to the Einstein field equations exhibit specific energy conditions, $T_v{}^v$ negative and ρ_Λ positive everywhere, which preferentially support the existence of FITHs [33]. Prime examples are the Reissner–Nordstrom (low electric charge) and Schwarzschild-de Sitter black holes, including their dynamical generalizations [24,34]. In such spacetimes, the standard configuration consists of concentric trapping horizons, with both the FOTH and the FITH enclosing the central singularity.

In an extremal case, FOTH and FITH merge onto a single trapping horizon. This condition is formally characterized by a vanishing geometric surface gravity, as presented in Appendix A. A third, more radical, scenario arises when both horizons disappear completely, exposing a naked singularity. Such cases raise profound theoretical challenges, as they represent a violation of the cosmic censorship conjecture, which is beyond the scope of the present work.

In summary, the existence of black holes with multiple horizons requires specific conditions that ensure the simultaneous presence of both the outer and inner horizons. When the black hole is perturbed, the positions of these horizons may shift, requiring a reexamination of the conditions that guarantee the existence of the black hole with a

well-defined boundary. In this work, we develop a systematic perturbative scheme for investigating accretion-induced shifts in the horizons of an accreting black hole.

3.2. General Model

Aiming at this dynamical analysis of the trapping horizons subjected to perturbations, an approximation scheme is developed in this section to simplify the metric near a surface $r = r_0$. We have seen that, in the appropriate coordinates of Equation (8), the metric tends to a Vaidya form near r_0. Moreover, we will show that, up to a first correction of the Misner–Sharp mass near r_0, the metric locally acquires a form that can be related to the Vaidya–de Sitter spacetime.

For the subsequent analysis, consider the parameter ϵ, defined as

$$\epsilon \equiv r - r_0 . \tag{20}$$

We will approximate the Misner–Sharp mass around $r = r_0$, treating ϵ/r_0 as a small parameter. Concretely, the Vaidya–de Sitter line element,

$$ds^2 = -\left\{1 - \frac{2}{r}\left[m(v) + \frac{4\pi r^3}{3}\rho_\Lambda\right]\right\}dv^2 + 2dvdr + r^2d\Omega^2 , \tag{21}$$

has its quasi-local mass approximated in the vicinity of r_0, $(r_0, r_0 + \epsilon)$, at first order in ϵ/r_0, as

$$M_{\text{MS}}(v,r) \approx M_{\text{MS}}(v,r_0) + 4\pi r_0^2 \epsilon \rho_\Lambda , \quad M_{\text{MS}}(v,r_0) = m(v) + \frac{4\pi r_0^3}{3}\rho_\Lambda . \tag{22}$$

The term $4\pi r_0^2 \epsilon$ corresponds to the (Euclidean) volume of a thin spherical shell of radius r_0 and thickness ϵ. Thus, the second term in the expansion of $M_{\text{MS}}(v,r)$ ($4\pi r_0^2 \epsilon \rho_\Lambda$) represents the energy contribution from the cosmological constant within this thin shell, providing a first-order correction to the Misner–Sharp mass. Within this approximation, the Vaidya–de Sitter geometry is characterized near r_0 by

$$ds^2 = -\left\{1 - \frac{2}{r}\left[m(v) + \frac{4\pi r_0^3}{3}\rho_\Lambda + 4\pi r_0^2 \epsilon \rho_\Lambda\right]\right\}dv^2 + 2dvdr + r^2d\Omega^2 . \tag{23}$$

More generally, using Equations (9)–(15) and keeping only the leading-order contribution of the energy–momentum tensor in the region $(r_0, r_0 + \epsilon)$, we obtain the following:

$$M_{\text{MS}}(v,r) \approx M_{\text{MS}}(v,r_0) - 4\pi r_0^2 \epsilon [T_v{}^v(v,r_0) - \rho_\Lambda] , \tag{24}$$

with $M_{\text{MS}}(v,r_0)$ determined by initial conditions and the flow $\mathcal{A}$ across r_0. This result implies that the metric can be approximated to a "Vaidya-dark energy form" around r_0, with an effective dynamical cosmological constant $\tilde{\Lambda}$ given by

$$\rho_{\tilde{\Lambda}}(v) \equiv -T_v{}^v(v,r_0) + \rho_\Lambda . \tag{25}$$

It follows that, given the condition

$$\epsilon \ll \left|\frac{\mathcal{B}(v,r_0)}{\mathcal{B}'(v,r_0)}\right| , \tag{26}$$

the Misner–Sharp mass in the vicinity of r_0 is approximated to the mass of a Vaidya geometry in a background dominated by a dynamical cosmological constant.

3.3. Perfect Fluid Model

A particularly interesting case from our previous results concerns the accretion of perfect fluids. More specifically, let us consider an energy–momentum tensor

$$T^{\mu\gamma} = (\rho + p)u^\mu u^\gamma + pg^{\mu\gamma} , \tag{27}$$

where the energy density ρ and pressure p are dynamical functions of both the time and radial coordinates, i.e., $\rho \equiv \rho(v,r)$ and $p \equiv p(v,r)$.

The 4-velocity u^μ of the fluid takes the form

$$u^\mu = \big[F(v,r),\, -G(v,r),\, 0,\, 0\big], \tag{28}$$

with the radial velocity (G) required to be a positive function. The v-component (F) is determined by the normalization condition $u_\mu u^\mu = -1$, yielding:

$$u^\mu = \left(\frac{e^{-\lambda}}{G + \sqrt{G^2 + 1 - \frac{2M_{\mathrm{MS}}}{r}}},\, -G,\, 0,\, 0 \right). \tag{29}$$

This is the general form for the 4-velocity of a radially ingoing perfect fluid in a spherically symmetric spacetime using the coordinates of Equation (2). Near a fixed r_0, the Misner–Sharp mass in Equation (29) can be approximated by Equation (24).

Using the chart of Equation (8), the relevant non-zero components of the energy–momentum tensor are written as

$$T_v{}^v = \frac{-\rho\sqrt{1 - \frac{2M_{\mathrm{MS}}}{r} + G^2} + pG}{\sqrt{1 - \frac{2M_{\mathrm{MS}}}{r} + G^2} + G} ,\quad T_r{}^v = \frac{e^{-\lambda+\lambda_0}(\rho + p)}{\left[G + \sqrt{G^2 + 1 - \frac{2M_{\mathrm{MS}}}{r}}\right]^2} ,\quad T_v{}^r = G(\rho + p)e^{\lambda-\lambda_0}\sqrt{1 - \frac{2M_{\mathrm{MS}}}{r} + G^2} , \tag{30}$$

with $\lambda_0 \equiv \lambda(v,r_0)$. From the previous development, the metric takes the form of a Vaidya-dark energy solution in the vicinity of the surface $r = r_0$, up to first-order corrections of ϵ/r_0 on M_{MS}. In the case of a perfect fluid, if r_0 is the position of the trapping horizon at a particular v, then the effective vacuum energy $\rho_{\tilde\Lambda}$ in Equation (25) (associated to an effective dynamical cosmological constant $\tilde\Lambda$) acquires the form:

$$\rho_{\tilde\Lambda}(v,r_0) = \frac{1}{2}[\rho(v,r_0) - p(v,r_0)] + \rho_\Lambda . \tag{31}$$

We emphasize that the near-horizon approximation,

$$M_{\mathrm{MS}}(v,r) \approx M_{\mathrm{MS}}(v,r_0) + 2\pi r_0^2 \epsilon[\rho(v,r_0) - p(v,r_0) + 2\rho_\Lambda] , \tag{32}$$

exhibits a leading-order correction determined solely by the physical scalars ρ, p and ρ_Λ. That is, this correction term is independent of any explicit coupling between the fluid and the geometry, such as kinematic terms (u^μ) or the metric itself ($g_{\mu\gamma}$).

4. Perturbative Scheme for Accretion

4.1. Perturbations near a Trapping Horizon

In the previous section, we developed a general approximation scheme for the Misner–Sharp mass, presented in Equation (24). This framework provides the specific form for a perfect fluid's energy–momentum tensor in Equation (32), valid near a trapping horizon. Within this scheme, the surface $r = r_0$ represents the position of the horizon at a fixed value

of the affine parameter, set as $v = 0$ for convenience. To fully characterize the metric in this neighborhood of r_0, $M_{\mathrm{MS}}(v, r_0)$ must be specified. However, this typically requires knowledge of the complete solution, which is generally not available. In this context, a perturbative approach proves particularly valuable, as it allows us to consider fluid accretion on a fixed, predetermined black-hole background.

The general framework of the perturbative scheme is given by a background metric $g_{\mu\gamma}^{(0)}$ that solves the Einstein Equation for a field $\phi^{(0)}$,

$$G_{\mu\gamma}\left[g_{\mu\gamma}^{(0)}\right] = 8\pi T_{\mu\gamma}\left[g_{\mu\gamma}^{(0)}, \phi^{(0)}\right] , \tag{33}$$

and the perturbation $g_{\mu\gamma}^{(1)}$ on the metric is produced by a field $\phi^{(1)}$ such that the Einstein Equation for the perturbed spacetime is given by

$$G_{\mu\gamma}\left[g_{\mu\gamma}^{(0)} + g_{\mu\gamma}^{(1)}\right] = 8\pi T_{\mu\gamma}\left[g_{\mu\gamma}^{(0)}, \phi^{(0)} + \phi^{(1)}\right] . \tag{34}$$

The energy–momentum tensor is determined by the test fluid approximation, requiring the matter fields on the right-hand side of Equation (34) to satisfy their equations of motion on the background spacetime. Nonetheless, backreaction effects on the metric are considered, as evidenced in the left-hand side.

Our framework analyzes the backreaction on the background Misner–Sharp mass. While reference [26] established conditions for the validity of a similar perturbation scheme, we propose two significant refinements. First, the fluid's dynamical degrees of freedom are preserved. Second, the systematic near-horizon expansion in our method facilitates the computation of higher-order corrections. This approach provides a controlled approximation scheme for studying backreaction effects while maintaining consistency with the dynamical evolution of the spacetime.

To analyze the behavior of the trapping horizon under a perturbation, we employ the Misner–Sharp mass decomposition within our perturbative framework,

$$M_{\mathrm{MS}}(v, r) = M_{\mathrm{MS}}^{(0)}(v, r) + M_{\mathrm{MS}}^{(1)}(v, r) , \tag{35}$$

which requires

$$\frac{M_{\mathrm{MS}}^{(1)}(v, r)}{M_{\mathrm{MS}}^{(0)}(v, r)} \ll 1 . \tag{36}$$

In Equation (35), the background and first-order contributions are given by the following:

$$M_{\mathrm{MS}}^{(0)}(v, r) = M_{\mathrm{MS}}^{(0)}(0, r_0) + \int_0^v \mathcal{A}^{(0)}(v', r_0)dv' + \int_{r_0}^r \mathcal{B}^{(0)}(v, r')dr' , \qquad T_{\mu\gamma}^{(0)} = T_{\mu\gamma}\left[g_{\mu\gamma}^{(0)}, \phi^{(0)}\right] , \tag{37}$$

$$M_{\mathrm{MS}}^{(1)}(v, r) = \int_0^v \mathcal{A}^{(1)}(v', r_0)dv' + \int_{r_0}^r \mathcal{B}^{(1)}(v, r')dr' , \qquad T_{\mu\gamma}^{(1)} = T_{\mu\gamma}\left[g_{\mu\gamma}^{(0)}, \phi^{(1)}\right] . \tag{38}$$

We have assumed that the accretion process begins strictly for $v > 0$, setting

$$M_{\mathrm{MS}}^{(1)}(0, r_0) = 0 . \tag{39}$$

That is, at $v = 0$, the Misner–Sharp mass evaluated at the initial position of the trapping horizon (r_0) is determined by the background alone.

A natural initial application for the perturbative scheme involves a Schwarzschild background [33], with mass parameter m and $\phi^{(0)} = 0$. In this case, the Misner–Sharp mass decomposes as

$$M_{\text{MS}}^{(0)}(v,r) = M_{\text{MS}}^{(0)} = m \, , \quad M_{\text{MS}}(v,r) = m + \int_0^v \mathcal{A}^{(1)}(v',r_0)dv' + \int_{r_0}^r \mathcal{B}^{(1)}(v,r')dr' \, . \quad (40)$$

As a more complex scenario, we consider a Reissner–Nordström background [33], with electric charge Q and $\phi^{(0)}$ representing the electric potential. In this case, the Misner–Sharp mass can be written as follows:

$$M_{\text{MS}}^{(0)}(v,r) = M_{\text{MS}}^{(0)}(r) = m - \frac{Q^2}{2r} \, , \quad M_{\text{MS}}(v,r) = m - \frac{Q^2}{2r} + \int_0^v \mathcal{A}^{(1)}(v',r_0)dv' + \int_{r_0}^r \mathcal{B}^{(1)}(v,r')dr' \, . \quad (41)$$

In the following section, we examine how accretion affects the trapping horizons of a Reissner–Nordström black hole.

4.2. Accretion-Induced Shifts in Trapping Horizons

To incorporate the approximation scheme of Section 3 into the perturbative framework, we perform a systematic near-horizon expansion in powers of ϵ, defined in Equation (20), analyzing three successive orders:

(Zeroth-order accreting solution) The exact solution at $\epsilon = 0$ from Equation (37), including metric perturbations at $\epsilon = 0$ from Equation (38):

$$M_{\text{MS}}^{[0]}(v,r) \equiv M_{\text{MS}}^{(0)}(v,r_0) + \bar{\mathcal{A}}^{(1)}(v,r_0) \, . \quad (42)$$

(First-order accreting solution) The full exact solution from Equation (37), including metric perturbations at $\epsilon = 0$ from Equation (38):

$$M_{\text{MS}}^{[1]}(v,r) \equiv M_{\text{MS}}^{(0)}(v,r) + \bar{\mathcal{A}}^{(1)}(v,r_0) \, . \quad (43)$$

(Full perturbation) Incorporating the contribution $\mathcal{B}^{(1)}$ evaluated at r_0:

$$M_{\text{MS}}^{[2]}(v,r) \equiv M_{\text{MS}}^{(0)}(v,r) + \bar{\mathcal{A}}^{(1)}(v,r_0) + \epsilon \mathcal{B}^{(1)}(v,r_0) \, . \quad (44)$$

In Equations (42)–(44), we have defined

$$\bar{\mathcal{A}}^{(1)}(v,r_0) \equiv \int_0^v \mathcal{A}^{(1)}(v',r_0)dv' \, . \quad (45)$$

Let r_0 denote the initial position of a trapping horizon. In the unperturbed Reissner–Nordström spacetime, its position is determined by

$$r_0 = m \pm \sqrt{m^2 - Q^2} \, , \quad (46)$$

with the usual extremal condition:

$$m \overset{\text{ext}}{=} |Q| \, , \qquad r_0 \overset{\text{ext}}{=} |Q| \, . \quad (47)$$

In what follows, we investigate small horizon shifts $\epsilon(v) \equiv r_H(v) - r_0$ induced by matter accretion.

Using the zeroth-order accreting solution of Equation (42), the perturbed Misner–Sharp mass takes the form:

$$M_{\mathrm{MS}}^{[0]}(v,r) = m + \bar{\mathcal{A}}^{(1)}(v,r_0) - \frac{Q^2}{2r_0} . \tag{48}$$

This leads to a time-dependent horizon shift:

$$\frac{r_H^{[0]}(v)}{2} = m - \frac{Q^2}{2r_0} + \bar{\mathcal{A}}^{(1)}(v,r_0) . \tag{49}$$

Extending to our first-order accreting solution of Equation (43), the Misner–Sharp mass becomes

$$M_{\mathrm{MS}}^{[1]}(v,r) = m + \bar{\mathcal{A}}^{(1)}(v,r_0) - \frac{Q^2}{2r} , \tag{50}$$

which generates shifts in the horizon as

$$\frac{r_H^{[1]}(v)}{2} = m - \frac{Q^2}{2r_H^{[1]}(v)} + \bar{\mathcal{A}}^{(1)}(v,r_0) . \tag{51}$$

This rational Equation (51) in $r_H^{[1]}(v)$ yields the exact solution:

$$r_H^{[1]}(v) = m + \bar{\mathcal{A}}^{(1)}(v,r_0) \pm \sqrt{\left[\bar{\mathcal{A}}^{(1)}(v,r_0)\right]^2 + m^2 - Q^2 + 2m\bar{\mathcal{A}}^{(1)}(v,r_0)} . \tag{52}$$

Note that, in this first-order approximation, the horizon position remains fixed for $v \leq 0$ as a consequence of assumption (39), reducing to Equation (46).

At this order of approximation, the extremal condition is given by

$$m \overset{\mathrm{ext}}{=} |Q| - \bar{\mathcal{A}}^{(1)}(v,r_0) , \tag{53}$$

with the corresponding horizon position obtained from Equation (52),

$$r_H^{[1]}(v) \overset{\mathrm{ext}}{=} |Q| . \tag{54}$$

Thus, it is found that the corrected condition for the existence of the trapping horizons is

$$\bar{\mathcal{A}}^{(1)}(v,r_0) \geq -m + |Q| , \tag{55}$$

for all values of v.

Since the initial condition $M_{\mathrm{MS}}(0,r_0) = M_{\mathrm{MS}}^{(0)}(0,r_0)$ implies $m \geq |Q|$, the inequality (55) is automatically satisfied for physical fluids obeying the traditional energy conditions. This suggests that matter influx alone can only drive an extremal horizon to split into distinct inner and outer horizons. That is, the influx of electrically neutral perfect fluid directly leads to the breakdown of the extremality condition (53). Furthermore, it also indicates that phantom-energy accretion (with $\bar{\mathcal{A}}^{(1)} < 0$) could violate this condition, leading to horizon disappearance.

So far, our analysis has not considered the contribution of the energy density. To include it, we use the full perturbation of Equation (44):

$$M_{\mathrm{MS}}^{[2]}(v,r) = m + \bar{\mathcal{A}}^{(1)}(v,r_0) - \frac{Q^2}{2r} + \epsilon \mathcal{B}^{(1)}(v,r_0) . \tag{56}$$

For a dust fluid, generalization discussed previously as $\rho_{\tilde{\Lambda}}$, the horizon position becomes the following:

$$\frac{r_H^{[2]}(v)}{2} = m - \frac{Q^2}{2r_H^{[2]}(v)} + \bar{\mathcal{A}}^{(1)}(v, r_0) + 2\pi r_0^2 \left[r_H^{[2]}(v) - r_0\right]\rho(v, r_0) . \tag{57}$$

The exact solution to Equation (57) is

$$r_H^{[2]}(v) = \frac{2\pi r_0^3 \rho(v, r_0) - \bar{\mathcal{A}}^{(1)}(v, r_0) - m \pm \sqrt{Q^2\left[4\pi r_0^2 \rho(v, r_0) - 1\right] + \left[\bar{\mathcal{A}}^{(1)}(v, r_0) + m - 2\pi r_0^3 \rho(v, r_0)\right]^2}}{4\pi r_0^2 \rho(v, r_0) - 1} . \tag{58}$$

The corrected extremal condition now incorporates energy density effects:

$$m \stackrel{\text{ext}}{=} -\bar{\mathcal{A}}^{(1)}(v, r_0) + 2\pi r_0^3 \rho(v, r_0) + \sqrt{Q^2\left[1 - 4\pi r_0^2 \rho(v, r_0)\right]} , \tag{59}$$

with the position of the extremal horizon given by

$$r_H^{[2]}(v) \stackrel{\text{ext}}{=} \frac{|Q|}{\sqrt{1 - A_0 \rho(v, r_0)}} , \qquad A_0 = 4\pi r_0^2 . \tag{60}$$

The framework is reliable for small perturbations, $\rho(v, r) \sim 0$. Hence, up to a first correction, the position of the trapping horizon of a perturbed extremal Reissner–Nordström black hole is given by

$$r_H^{[2]}(v) \stackrel{\text{ext}}{=} |Q|\left[1 + \frac{A_0 \rho(v, r_0)}{2}\right] . \tag{61}$$

Some key advances of our perturbative approach are discussed. The result (52) shows that retaining second-order influx terms in the square root induces first-order corrections to the extremal condition, leading to the necessity of a revised analysis of the existence criteria for trapping horizons. Also, result (58) incorporates energy density effects, generating a corrected extremal condition with additional terms, as well as a shifted horizon position for extremal Reissner–Nordström black holes. Finally, our perturbative approach produced higher order corrections than those of [26].

This section presents the main results of our work. However, we further examine the properties of future inner trapping horizons, given their profound theoretical implications.

5. On the Presence of Future Inner Trapping Horizons

As established in Section 3.1, future inner trapping horizons are found in many solutions. However, their presence implies that the standard black-hole boundary definition via a future outer trapping horizon must now be complemented with additional existence conditions. This requires a particularly careful treatment when studying perturbations on extremal and near-extremal configurations, as was carried out in the previous section.

The existence of inner horizons also leads to a variety of potential theoretical challenges: as possible Cauchy horizons, raising questions regarding the predictability of general relativity [35]; and as unstable loci [36], most notably resulting in the mass inflation phenomenon [37–39]. Recent work has reinterpreted these phenomena for FITHs in dynamical spacetimes [40], moving beyond the traditional analysis based on stationary black holes.

It is thus remarkable that we can identify small metric corrections that incorporate repulsive effects, which can eliminate the inner horizon in some scenarios. This mechanism generates a secondary FOTH within the FITH. We have observed that the smaller the FITH is, the easier it is to destroy it. For sufficiently strong corrections, this inner FOTH can

completely cancel out the FITH, leaving only the outer horizon as the boundary of the black hole. More precisely, we consider specific deviations of the form

$$M_{\text{MS}} \longrightarrow M_{\text{MS}} + \alpha r^{-\beta} \,, \tag{62}$$

where α is positive and β is a non-negative integer. These corrections are well motivated by several works in the literature, particularly spacetimes incorporating quantum gravity effects. For instance, similar terms emerge as one-loop corrections in gravitational effective field theories (see [41] and references therein). As a concrete scenario, the FOTH of a Schwarzschild can be shifted (but never destroyed) for any pair of (α, β). For a Reissner–Nordstrom black hole,

$$M_{\text{MS}} = m - \frac{Q^2}{2r} \longrightarrow m - \frac{Q^2}{2r} + \alpha r^{-\beta} \,. \tag{63}$$

As shown in Figure 1, there are qualitatively different repulsive corrections on the metric of a Reissner–Nordström black hole, which favors the vanishing of the FITH for increasing values of β. In fact, virtually undetectable corrections to the metric by an exterior observer can be sufficient to make the inner horizon vanish.
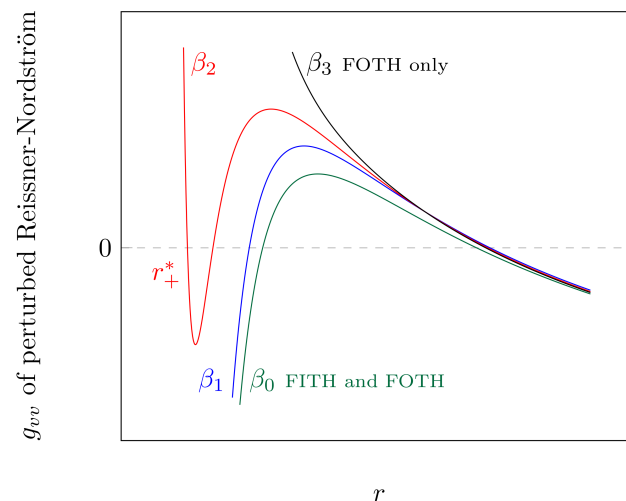

Figure 1. General representation of the metric function g_{vv} of a pure Reissner–Nordström black hole (β_0) with (FITH) $r_- \sim 0$ corrected by the same α and increasing values of β: from β_1 to β_3. The quantity r_+^* denotes a secondary FOTH that is formed between the singularity and the FITH by the correction β_2.

The perturbative analysis developed in the previous section can be straightforwardly extended to Reissner–Nordström with this correction. For several values of the parameters α and β, the solution admits a single (outer) trapping horizon, defining its boundary. This simplifies the perturbative treatment and avoids potential instabilities arising from the presence of the inner horizon.

6. Final Remarks

In this work, we have investigated the dynamics of future trapping horizons of spherically symmetric spacetimes using ingoing Eddington–Finkelstein coordinates. We have shown that their exact evolution is described by an integral form of Hayward's first law. Our results demonstrate the important role of quasi-local quantities, in particular trapping horizons and the Misner–Sharp mass, in characterizing the accretion-induced evolution of black holes. These tools are particularly valuable when exact solutions incorporating backre-

action effects are not available and when going beyond standard test-fluid approximations is desirable.

To consider backreaction in our analysis, we have implemented a near-horizon approximation scheme that systematically captures first-order corrections of the Vaidya-dark energy type. This framework is particularly useful for simplifying the analysis of perfect fluids near trapping horizons since the leading-order corrections depend only on the fluid's energy density ρ and pressure p, with no explicit dependence on either the fluid's velocity field or the background metric components. This simplification arises because, in the first correction, the interaction of the fluid with the geometry is fully encoded in the stress-energy tensor via ρ and p.

Building on this foundation, our perturbative framework extends previous results by systematically incorporating higher-order corrections. The formalism is constructed in a background-independent manner and subsequently applied to study accretion onto a Reissner–Nordström black hole. Our analysis reveals a hierarchy of horizon displacements, with distinct perturbative orders producing characteristically different modifications to both the horizon location and the extremality conditions. Significantly, we find that momentum influx (from non-exotic matter) preserves the coordinate location of an extremal horizon, serving only to bifurcate it into separate inner and outer components. Energy density contributions, by contrast, produce measurable shifts of the extremal horizon position.

The generality of our framework, combined with its systematic perturbative construction, opens up several promising directions for future research. We have observed that certain repulsive corrections in the metric are able to eliminate an inner horizon, thus avoiding the additional theoretical challenges they pose. It would be of significant interest to investigate this effect within a perturbative framework. However, such an analysis would likely require going beyond the localized perturbations used in accretion models. Furthermore, since these corrections directly impact the Misner–Sharp mass, they yield new results for quasi-local versions of black-hole thermodynamics. This suggests the need for further investigation into the effects of metric corrections on horizon structure.

Moreover, it is possible to implement our methodology to outgoing Eddington–Finkelstein coordinates, which can be used to model Hawking evaporation [25,42,43]. Also, in this case, the formalism could be applied to the study of the dynamics of past cosmological horizons, which are those of fast-expanding cosmologies. Since the perturbative approach developed here is valid close to a trapping horizon, it naturally enables the investigation of dynamical configurations in near-extremal regimes. This is particularly true for spacetimes like Vaidya–de Sitter and its generalizations. Another extension of this work involves incorporating higher-order perturbations, for which a better formalization of our theoretical framework is required. Research is being conducted along these lines.

Appendix A. Future Trapping Horizons

The boundary of a black hole is considered in this work to be a future outer trapping horizon (FOTH), which is characterized by the conditions that are made explicit in this appendix. The brief presentation starts with the expansion scalar, which measures the rate of change of the transverse metric $h_{\mu\gamma}$ along the generators k of a null[1] congruence,

$$\theta_k = \frac{1}{\sqrt{h}} \partial_k \sqrt{h} \, , \tag{A1}$$

where h denotes the determinant of the transverse metric $h_{\mu\gamma}$:

$$h \equiv \det(h_{\mu\gamma}) \, , \quad h_{\mu\gamma} \equiv g_{\mu\gamma} + l_\mu n_\gamma + n_\mu l_\gamma \, . \tag{A2}$$

The tensor $h_{\mu\gamma}$ projects vectors on the cross-sectional surface orthogonal to the null vector fields l^μ and n^μ.

In this work, we consider the metric of a spherically symmetric geometry in the general form of Equation (2). For the null fields, we take the ingoing and outgoing vectors:

$$n = -\partial_r \, , \tag{A3}$$

$$l = e^{-\lambda} \partial_v + \frac{1}{2}\left(1 - \frac{2M_{\mathrm{MS}}}{r}\right)\partial_r \, . \tag{A4}$$

It can be checked from Equation (A2) that the area element of the cross-sectional surface orthogonal to both l^μ and n^μ is

$$\sqrt{h} = r^2 \sin\theta \, , \tag{A5}$$

which characterizes a 2-sphere. And, for the expansion scalar (A1),

$$\theta_n = -2r\sin\theta \, , \tag{A6}$$

$$\theta_l = \frac{1}{r}\left(1 - \frac{2M_{\mathrm{MS}}}{r}\right) \, . \tag{A7}$$

By definition (14), there is a future trapping horizon at $r_H(v)$ if

$$r_H(v) = 2M_{\mathrm{MS}} \, . \tag{A8}$$

This structure is characterized by the sign of $\mathcal{L}_n \theta_l$ at r_H, where $\mathcal{L}$ denotes the Lie derivative. For a FOTH we have, for all v,

$$\mathcal{L}_n \theta_l\big|_{r_H(v)} < 0 \quad \Longleftrightarrow \quad \mathcal{B}(v, r_H(v)) \equiv \frac{\partial M_{\mathrm{MS}}}{\partial r}\bigg|_{r_H(v)} < \frac{1}{2} \, . \tag{A9}$$

And for it to be a future inner trapping horizon (FITH), which is a typical boundary of a contracting spacetime,

$$\mathcal{L}_n \theta_l\big|_{r_H(v)} > 0 \quad \Longleftrightarrow \quad \mathcal{B}(v, r_H(v)) \equiv \frac{\partial M_{\mathrm{MS}}}{\partial r}\bigg|_{r_H(v)} > \frac{1}{2} \, . \tag{A10}$$

When $\mathcal{B} = 1/2$, which suggests FOTH and FITH merging, we have an extremal trapping horizon. This is equivalently characterized by the vanishing of the geometric surface gravity:

$$\kappa_G \equiv \frac{1}{2\sqrt{\det|g_{ab}|}} \partial_c \left(\sqrt{\det|g_{ab}|}\, g^{cd} \partial_d r\right) = -\partial_r\left(\frac{M_{\mathrm{MS}}}{r}\right) \, , \tag{A11}$$

with g_{ab} defined after Equation (17), and the second equality given by evaluation in the coordinates of Equation (2), where Latin indexes stand for v and r.

There are two other types of trapping horizons: the past (outer and inner) ones. However, these are covered by outgoing Eddington–Finkelstein coordinates, which are not as useful for investigating the dynamics of black-hole accretion.

Note

1.   The investigation of null congruences is useful for the study of trapping horizons, but the expansion scalar can also be defined for timelike congruences.

References

1.   Krishnan, B. Fundamental properties and applications of quasi-local black hole horizons. *Class. Quant. Grav.* **2008**, *25*, 114005. [CrossRef]
2.   Jaramillo, J.L.; Gourgoulhon, E. Mass and angular momentum in general relativity. In *Mass and Motion in General Relativity*; Blanchet, L., Spallicci, A., Whiting, B., Eds.; Springer: Dordrecht, The Netherlands, 2011; pp. 87–124.
3.   Hayward, S.A. General laws of black-hole dynamics. *Phys. Rev. D* **1994**, *49*, 6467. [CrossRef] [PubMed]
4.   Misner, C.; Sharp, D. Relativistic equations for adiabatic, spherically symmetric gravitational collapse. *Phys. Rev.* **1964**, *136*, B571. [CrossRef]
5.   Hernandez, W.C.; Misner, C.W. Observer time as a coordinate in relativistic spherical hydrodynamics. *Astrophys. J.* **1966**, *143*, 452. [CrossRef]
6.   Ashtekar, A.; Krishnan, B. Isolated and dynamical horizons and their applications. *Living Rev. Rel.* **2004**, *7*, 10. [CrossRef]
7.   Abreu, G.; Visser, M. Kodama time: Geometrically preferred foliations of spherically symmetric spacetimes. *Phys. Rev. D* **2010**, *82*, 044027. [CrossRef]
8.   Booth, I. Black-hole boundaries. *Can. J. Phys.* **2005**, *83*, 1073–1099. [CrossRef]
9.   Fodor, G.; Nakamura, K.; Oshiro, Y.; Tomimatsu, A. Surface gravity in dynamical spherically symmetric spacetimes. *Phys. Rev. D* **1996**, *54*, 3882. [CrossRef]
10.   Nielsen, A.B. Black holes and black hole thermodynamics without event horizons. *Gen. Relativ. Gravit.* **2009**, *41*, 1539–1584. [CrossRef]
11.   Nielsen, A.B.; Yeom, D. Spherically symmetric trapping horizons, the Misner-Sharp mass and black hole evaporation. *Int. J. Mod. Phys. A* **2009**, *24*, 5261–5285. [CrossRef]
12.   Nielsen, A.B.; Yoon, J.H. Dynamical surface gravity. *Class. Quant. Grav.* **2008**, *25*, 085010. [CrossRef]
13.   Faraoni, V. Embedding black holes and other inhomogeneities in the universe in various theories of gravity: A short review. *Universe* **2018**, *4*, 109. [CrossRef]
14.   Visser, M. Physical observability of horizons. *Phys. Rev. D* **2014**, *90*, 127502. [CrossRef]
15.   McVittie, G.C. The mass-particle in an expanding universe. *Mon. Not. R. Astron. Soc.* **1933**, *93*, 325–339. [CrossRef]
16.   Carrera, M.; Giulini, D. Generalization of McVittie's model for an inhomogeneity in a cosmological spacetime. *Phys. Rev. D* **2010**, *81*, 043521. [CrossRef]
17.   Lake, K.; Abdelqader, M. More on McVittie's Legacy: A Schwarzschild-de Sitter black and white hole embedded in an asymptotically ΛCDM cosmology. *Phys. Rev. D* **2011**, *84*, 044045. [CrossRef]
18.   Faraoni, V.; Moreno, A.F.Z.; Prain, A. The charged McVittie spacetime. *Phys. Rev. D* **2014**, *89*, 103514. [CrossRef]
19.   Maciel, A.; Guariento, D.C.; Molina, C. Cosmological black holes and white holes with time-dependent mass. *Phys. Rev. D* **2015**, *91*, 084043. [CrossRef]
20.   Ruiz, F.; Molina, C.; Lima, J.A.S. Dynamical model for primordial black holes. *Phys. Rev. D* **2020**, *102*, 123516. [CrossRef]
21.   Thakurta, S.N.G. Kerr metric in an expanding universe. *Indian J. Phys. B* **1981**, *55*, 304–310.
22.   Vaidya, P.C. The gravitational field of a radiating star. *Proc. Indian Acad. Sci. Sect. A* **1951**, *33*, 264–276. [CrossRef]
23.   Vaidya, P.C. 'Newtonian' time in general relativity. *Nature* **1953**, *171*, 260–261. [CrossRef]
24.   Mallett, R.L. Radiating Vaidya metric imbedded in de Sitter space. *Phys. Rev. D* **1985**, *31*, 416. [CrossRef] [PubMed]
25.   Campos, T.L.; Molina, C.; Lima, J.A.S. Black-hole evaporation for cosmological observers. *arXiv* **2024**, arXiv:2411.08114.
26.   Babichev, E.; Dokuchaev, V.; Eroshenko, Y. Backreaction of accreting matter onto a black hole in the Eddington-Finkelstein coordinates. *Class. Quant. Grav.* **2012**, *29*, 115002. [CrossRef]
27.   Bardeen, J.M. Black holes do evaporate thermally. *Phys. Rev. Lett.* **1981**, *46*, 382. [CrossRef]
28.   Hayward, S.A. Gravitational energy in spherical symmetry. *Phys. Rev. D* **1996**, *53*, 1938. [CrossRef]
29.   Hayward, S.A. Unified first law of black-hole dynamics and relativistic thermodynamics. *Class. Quant. Grav.* **1998**, *15*, 3147. [CrossRef]

30. Hayward, S.A.; Di Criscienzo, R.; Nadalini, M.; Vanzo, L.; Zerbini, S. Local Hawking temperature for dynamical black holes. *Class. Quant. Grav.* **2009**, *26*, 062001. [CrossRef]

31. Faraoni, V. *Cosmological and Black Hole Apparent Horizons*; Springer: Berlin/Heidelberg, Germany, 2015. [CrossRef]

32. Kodama, H. Conserved energy flux for the spherically symmetric system and the backreaction problem in the black hole evaporation. *Prog. Theor. Phys.* **1980**, *63*, 1217–1228. [CrossRef]

33. Griffiths, J.; Poloský, J. *Exact Space-Times in Einstein's General Relativity*; Cambridge University Press: Cambridge, UK, 2009. [CrossRef]

34. Bonnor, W.B.; Vaidya, P.C. Spherically symmetric radiation of charge in Einstein-Maxwell theory. *Gen. Relativ. Gravit.* **1970**, *1*, 127–130. [CrossRef]

35. Penrose, R. Structure of space-time. In *Battelle Rencontres—1967 Lectures in Mathematics and Physics*; DeWitt, C.M., Wheeler, J.A., Eds.; W. A. Benjamin: Seattle, WA, USA, 1968; pp. 121–235.

36. Matzner, R.; Zamorano, N.; Sandberg, V. Instability of the Cauchy horizon of Reissner-Nordström black holes. *Phys. Rev. D* **1979**, *19*, 2821. [CrossRef]

37. Poisson, E.; Israel, W. Internal structure of black holes. *Phys. Rev. D* **1990**, *41*, 1796. [CrossRef] [PubMed]

38. Ori, A. Inner structure of a charged black hole: An exact mass-inflation solution. *Phys. Rev. Lett.* **1991**, *67*, 789. [CrossRef]

39. Di Filippo, F.; Carballo-Rubio, R.; Liberati, S.; Pacilio, C.; Visser, M. On the inner horizon instability of non-singular black holes. *Universe* **2022**, *8*, 204. [CrossRef]

40. Carballo-Rubio, R.; Filippo, F.; Liberati, S.; Visser, M. Mass inflation without Cauchy horizons. *Phys. Rev. Lett.* **2024**, *133*, 181402. [CrossRef]

41. Bargueño, P.; Medina, S.; Nowakowski, M.; Batic, D. Quantum-mechanical corrections to the Schwarzschild black-hole metric. *Europhys. Lett.* **2017**, *117*, 60006. [CrossRef]

42. Hiscock, W. Models of evaporating black holes. I. *Phys. Rev. D* **1981**, *23*, 2813. [CrossRef]

43. Hiscock, W. Models of evaporating black holes. II. Effects of the outgoing created radiation. *Phys. Rev. D* **1981**, *23*, 2823. [CrossRef]